Technical Report

Construction and Application of Machine-Learning Interatomic Potentials for Materials Design

Kazuma ITO*

Abstract

The demand for higher-strength steel materials is increasing in pursuit of carbon neutrality. In addition to conventional experiment-driven approaches, the application of atomistic computational science methods is highly effective for the development of novel high-strength steels. This paper reports Nippon Steel Corporation's recent efforts to apply such methods to steel materials development, including: (1) the construction of a highly accurate and transferable machine-learning interatomic potential (MLIP) for α-Fe, and (2) the non-empirical prediction of hydrogen diffusion coefficients in alloy systems using MLIP.

1. Introduction

Steel materials are used in various applications such as automobiles, construction, and industrial machinery, making them one of the most important materials. They are primarily composed of Fe and C, containing alloying elements like Mn, Si, and Al, as well as impurity elements like P and S. In addition to these chemical compositions, desired material properties are achieved by controlling the heat treatment process. Steel materials are generally polycrystalline, containing interfaces between grains with different crystal orientations, known as grain boundaries. Many alloying and impurity elements tend to enrich at these grain boundaries due to differences in atomic radius and chemical affinity with iron, a phenomenon called grain boundary segregation. Particularly in steel materials, it has long been known that specific elements like P and S segregate at grain boundaries, causing intergranular cracking and degrading mechanical properties and manufacturability—a phenomenon known as intergranular embrittlement.[1] Intergranular embrittlement has frequently hindered the application of steel materials as structural materials.

Achieving carbon neutrality by 2050 demands further increases in strength for steels used in various applications.[2] For example, in automotive steel sheets, the need for higher strength is intensifying to achieve vehicle body weight reduction while ensuring collision safety, driving the development of new high-strength steels.[3] Increased strength is achieved by inhibiting the slip motion of dislocations—the agents of plastic deformation—within grains. This inhibition occurs through alloying elements and the precipitates they form. When deformation within grains is hindered, deformation concentrates at grain boundaries, making mechanical properties increasingly dependent on grain boundary characteristics. Consequently, as strength increases, grain boundary embrittlement may occur even at levels of embrittling elements (P, S, Mn, H, etc.) that were previously not problematic.[4] Among these, suppressing embrittlement caused by hydrogen (H) introduced during steel manufacturing or in service environments, known as hydrogen embrittlement, is one of the most critical challenges.[2] Specifically, intergranular cracking due to intergranular embrittlement occurs at the so-called general grain boundaries. These boundaries constitute the majority of grain boundaries and possess complex atomic structures lacking specific crystallographic symmetry or regularity.[5] Therefore, developing high-strength steel requires material design that enhances strength while suppressing intergranular cracking at general grain boundaries.

However, grain boundaries are minute regions only a few atomic layers wide, making them difficult to observe even with the most advanced analytical techniques.[5] Furthermore, hydrogen, being a light element, is particularly challenging to analyze, making it extremely difficult to experimentally investigate its behavior within steel.[6] Consequently, it is difficult to obtain the insights needed for the aforementioned material design using experimental methods alone.

Against this backdrop, numerous studies have been conducted using atomic-level computational methods such as first-principles calculations based on density functional theory (DFT) (hereafter referred to as DFT calculations) and molecular dynamics analysis based on empirical interatomic potentials.[5, 7] Nippon Steel Corpora-

* Dr. Eng., Senior Researcher, Materials Characterization Research Lab., Advanced Technology Research Laboratories
20-1 Shintomi, Futtsu City, Chiba Pref. 293-8511

tion has also conducted fundamental research on grain boundaries and hydrogen embrittlement[8–10] using DFT calculations and molecular dynamics analysis. For example, DFT calculations have been used to investigate the segregation tendencies of various alloying elements[11–13] and their effects on grain boundary strength[14–16] in well-symmetric grain boundaries (hundreds of atoms in size), which are manageable and have relatively low computational costs. Furthermore, using empirical interatomic potentials that enable analysis of large-scale systems (millions of atoms) with low computational cost, investigations of grain boundary segregation behavior in general grain boundaries have been conducted.[17–19]

While these atomic-level computational methods are useful for fundamental research such as elucidating mechanisms, applying them to steel material development is not straightforward. Specifically, DFT calculations non-empirically compute atomic structure energies and interatomic forces based on electronic state calculations. While this offers the advantage of handling arbitrary elements, it also incurs high computational costs and is limited to extremely small computational domains of a few hundred atoms. Consequently, for instance, crack initiation at typical grain boundaries—critical in high-strength steel development—cannot be addressed due to computational cost constraints. Furthermore, dynamic factors, such as hydrogen diffusion near grain boundaries during deformation, which are presumed important in hydrogen embrittlement, are difficult to handle. In contrast, molecular dynamics analysis using empirical interatomic potentials can address crack initiation at typical grain boundaries due to its lower computational cost. However, empirical atomic potentials are generally created by fitting a few parameters of relatively simple function systems to reproduce a small number of material properties, such as lattice constants, elastic moduli, and cohesive energies. Consequently, they often fail to reproduce even the α-Fe grain boundary energy or the dynamics of atoms near grain boundaries with sufficient accuracy.[20] Furthermore, due to their origin in simple function systems, they lack flexibility, making it fundamentally difficult to construct high-precision interatomic potentials for ternary systems and beyond. Consequently, they cannot adequately account for the effects of C and other elements present in high-strength steels.

Recently, a breakthrough in interatomic potential construction has occurred with the proposal of machine-learning interatomic potential (MLIP), which has been applied to various material systems and demonstrated its validity.[21, 22] MLIP constructs interatomic potentials by using DFT calculations to compute various atomic structures, their energies, and the forces acting on each atom as training data. By appropriately selecting training data and constructing MLIP, it becomes theoretically possible to perform large-scale calculations on multi-component systems while maintaining the accuracy of DFT calculations. This holds potential for application in material design for high-strength steel development. However, it has been pointed out that MLIP, not being based on a physical model, exhibits a significant drop in accuracy for atomic structures corresponding to the so-called extrapolation region not included in the training data, and can sometimes cause non-physical behavior.[23] Particularly for atomic potentials, determining whether a region corresponds to an extrapolation region is not straightforward. For instance, constructing an MLIP capable of high-accuracy reproduction for systems containing complex atomic structures—such as typical grain boundaries and their deformation/fracture behavior—or systems with diverse elemental configurations formed by multiple alloying elements is challenging. Consequently, numerous challenges remain to be addressed for applying MLIPs to materials development.[24]

This report describes Nippon Steel's efforts toward steel material development using atomic-level calculation methods, specifically: 1) the construction of a highly accurate and transferable MLIP for α-Fe,[25,26] and 2) the non-empirical prediction of hydrogen diffusion coefficients in alloy systems using the constructed high-accuracy MLIP.[27]

2. Construction of a Highly Accurate and Transferable MLIP for α-Fe[25, 26]

Previous attempts to construct an α-Fe MLIP included not only α-Fe bulk but also dislocations represented by a few hundred atoms or less, highly symmetric grain boundaries, low-index surfaces, and other lattice defects, along with structures disturbed by these defects, in the training data to build a versatile MLIP.[28] On the other hand, it was assumed that conventional MLIP construction methods could not achieve sufficient accuracy for general grain boundaries, which are important in high-strength steel development. This is because general grain boundaries lack specific crystallographic symmetry and consist of complex and diverse atomic structures.

Therefore, we worked on constructing a machine learning potential with DFT-level accuracy for the grain boundary energy, atomic structure, and dynamics of arbitrary grain boundaries, including general grain boundaries.[26] As shown in **Fig. 1**(a), we used a learning dataset that included not only the conventional learning dataset for the bulk structure of α-Fe but also an additional dataset called RANDSPG,[29] which consists of diverse atomic structures generated mechanically and in large quantities based on crystal space groups. Furthermore, we adopted the moment tensor potential (MTP),[30] which offers an excellent balance between accuracy and computational cost, as the MLIP format. The computational accuracy of the obtained MLIP for general grain boundaries was evaluated by direct comparison with DFT calculations on cells extracted from the grain boundary vicinity of a nanoscale polycrystal obtained through relaxation using molecular dynamics calculations with the constructed MLIP, as shown in Fig. 1(b). For comparison, the accuracy of MLIPs from previous studies and empirical interatomic potentials was also evaluated. However, due to the high computational cost of DFT calculations, direct accuracy comparison with DFT could only be applied to a subset of grain boundary structures. Therefore, an evaluation using the extrapolation grade of the local atomic environment based on active learning methods was also performed. The extrapolation grade can be evaluated using the constructed MLIP. It numerically assesses whether an arbitrary atomic structure in the learning dataset used to build the MLIP corresponds to its interpolation region or its extrapolation region.[31] Consequently, this MLIP-based evaluation requires significantly lower computational cost than DFT verification and enables accuracy assessment for all atoms in the nanoscale polycrystal.

The accuracy evaluation results from direct comparison with DFT showed that the MLIP from previous research,[28] which was previously considered the most accurate for grain boundaries, exhibited an error of 139.3 meV/Å for atoms near general grain boundaries compared to DFT calculations, approximately twice that observed for α-Fe bulk. Therefore, general grain boundaries may correspond to the extrapolation region in the MLIP from previous studies. In contrast, the constructed MLIP demonstrated extremely high accuracy, with an error for atoms near general grain boundaries of 81.1 meV/Å, equivalent to the error for α-Fe bulk.[26] Further-

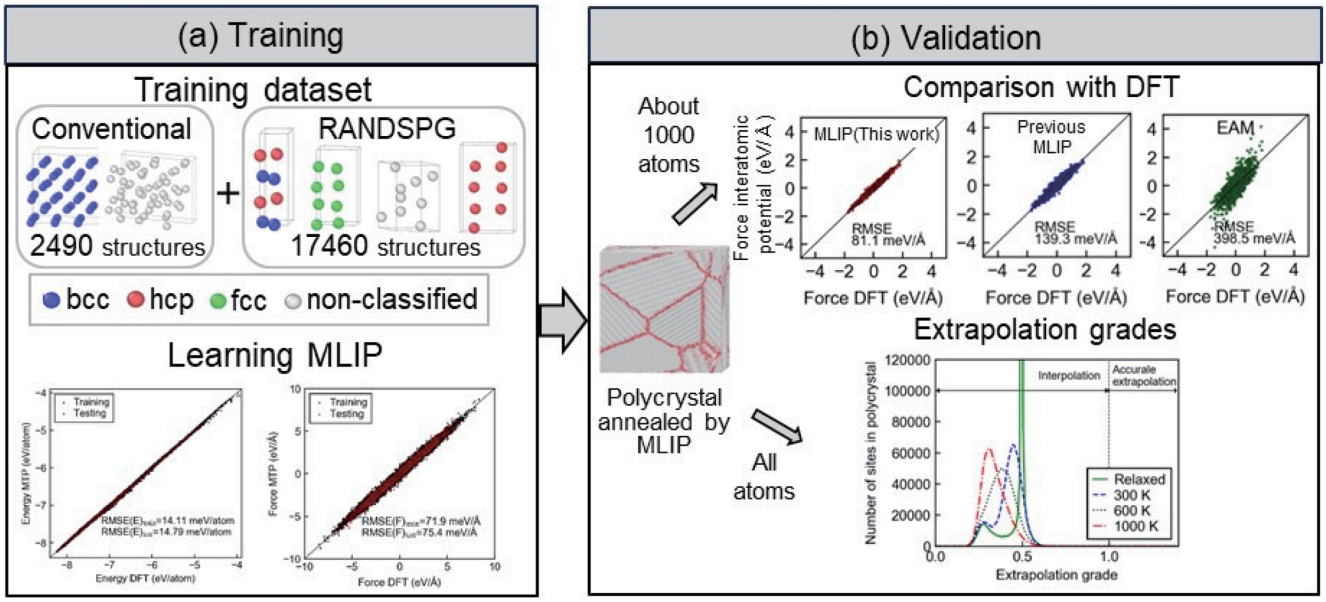

Fig. 1 Construction of a machine-learning interatomic potential (MLIP) for α-Fe[26]
(a) Training dataset used for MLIP construction and fitting results, (b) Validation procedure for the constructed MLIP
Accuracy of each interatomic potential in reproducing the forces on atoms near general grain boundaries calculated by DFT calculations. For comparison, the accuracy of an empirical interatomic potential (denoted as EAM) is also shown.

more, evaluation based on the extrapolation grade showed that the extrapolation grade was less than 1 for all atoms in the nanoscale polycrystal. This indicates that all atoms are within the interpolation region of the constructed MLIP, where high accuracy is expected[32] (see Fig. 1 (b)).

Furthermore, using the constructed MLIP in large-scale molecular dynamics simulations, we calculated the average grain boundary energy of α-Fe polycrystals—an important property difficult to determine directly experimentally. The resulting average grain boundary energy was 1.57 J/m^2, in good agreement with the recently estimated grain boundary energy for general α-Fe grain boundaries based on experimental results[32] (see **Fig. 2**). As described above, the constructed MLIP was found to be extremely accurate even for general grain boundaries composed of complex and diverse atomic structures.

Furthermore, we verified the computational accuracy of the constructed MLIP for the deformation and fracture behavior of nanoscale polycrystals.[25] Molecular dynamics calculations using the constructed MLIP were performed for uniaxial tensile loading of nanoscale polycrystals. We then comprehensively evaluated the extrapolation grade for approximately 660 000 atoms contained within the atomic structures generated during the uniaxial tensile process. The atomic structures observed during the uniaxial tensile process included deformed general grain boundaries, nucleation of lattice defects such as dislocations and deformed twins originating from grain boundaries, slip motion of dislocations and growth of deformed twins, as well as crack initiation and propagation (**Fig. 3** (a)). Consequently, the structures encompass complex and diverse atomic configurations related to these phenomena. Since an extrapolation grade of 2 or higher indicates insufficiently learned structures, Fig. 3 (b) plots the number of atoms judged to have an extrapolation grade of 2 or higher versus strain amount. The results show that for each strain level, only a few atoms at most exist among approximately 660 000 atoms with an extrapolation grade of 2 or higher. The computational accuracy of MLIP for these atoms was evaluated

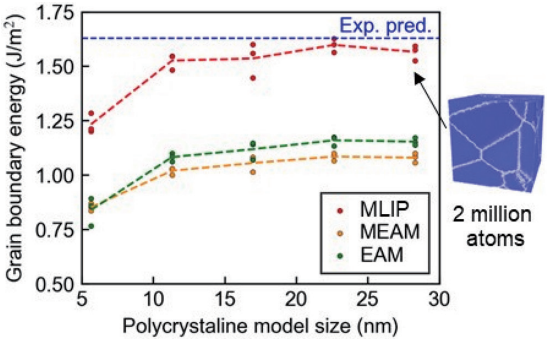

Fig. 2 Comparison between the average grain boundary energy of polycrystals calculated using the constructed MLIP and the experimental values[32]
The atomic structure model of the nanocrystalline polycrystal used in the calculations is also shown. For comparison, results obtained using conventional interatomic potentials (denoted as EAM and MEAM) are also presented.

by direct comparison with DFT, and the error was within an acceptable level. These results demonstrate that the constructed MLIP for α-Fe exhibits high accuracy not only for general grain boundaries but also for their deformation and fracture behavior, making it highly adaptable for various applications.

Using the constructed MLIP, large-scale molecular dynamics simulations clarified the grain size dependence of deformation and fracture behavior in nanoscale polycrystals (**Fig. 4**).[25] Here, molecular dynamics calculations were performed on a nanoscale polycrystal comprising approximately 5 million atoms using the Fugaku supercomputer, representing the largest-scale analysis of MLIP calculations for metallic materials to our knowledge. Furthermore, constructing an MLIP with such high accuracy for general grain boundaries and their deformation/fracture behavior, as achieved here, is unprecedented for other metallic systems.[24] The MLIP construction method used in this study is also applicable to other metallic materi-

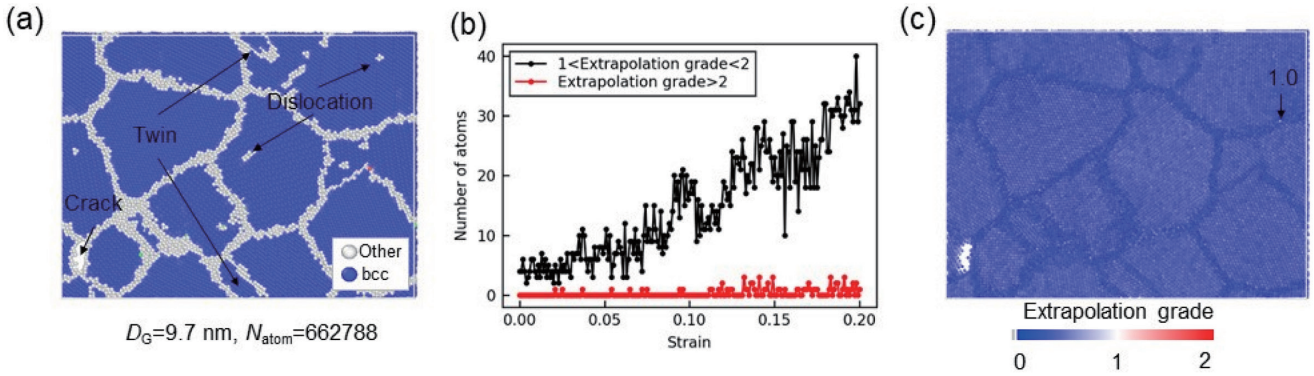

Fig. 3 Computational accuracy of the constructed MLIP in predicting the deformation and fracture behavior of nanocrystalline polycrystals[25]
(a) Atomic structure at 20% strain, (b) Strain dependence of the extrapolation grade, where atoms with an extrapolation grade exceeding 2 are considered to represent insufficiently sampled atomic configurations. (c) Color map of the extrapolation grade for each atom at 20% strain

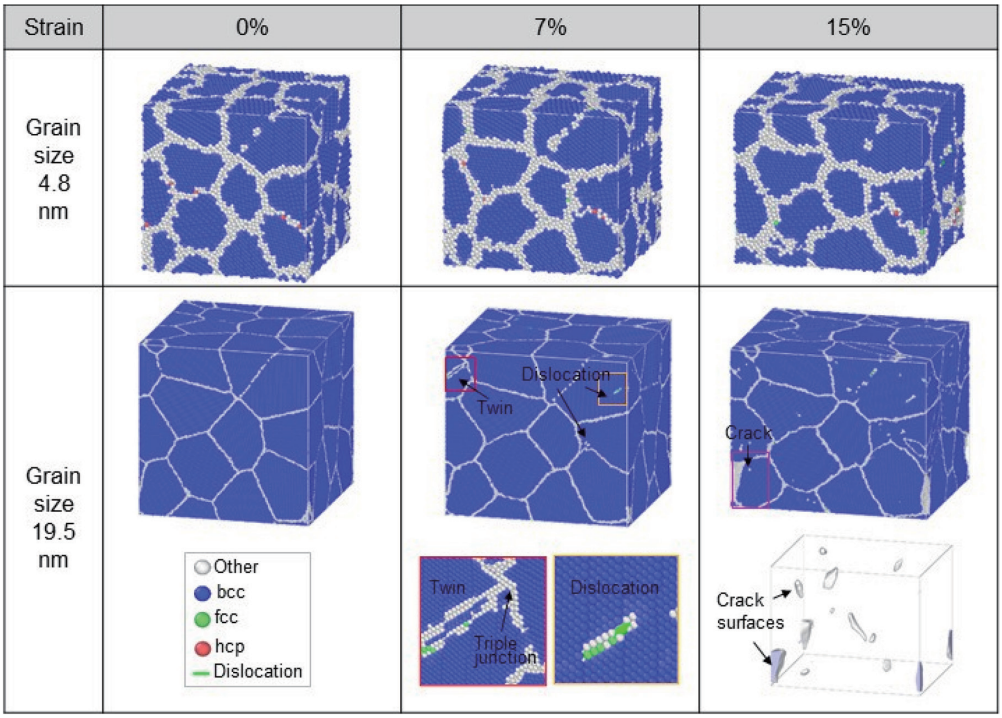

Fig. 4 Changes in atomic structure and crack morphology of nanocrystalline polycrystals with average grain sizes of 4.8 nm and 19.5 nm under increasing strain[25]
The crystal structure of each atom is indicated by color.

als. Therefore, this investigation is significant as it proposes a method for constructing high-accuracy, highly adaptable MLIPs.

As described above, by appropriately acquiring training datasets and constructing MLIPs, high-accuracy MLIPs applicable to various purposes can be obtained. This enables high-accuracy, large-scale analyses that were previously impossible.

3. Non-Empirical Prediction of Hydrogen Diffusion Coefficients in Alloy Systems via High-Precision MLIP Construction[27]

As mentioned earlier, resolving hydrogen embrittlement is a critical challenge in steel development. Hydrogen penetrates steel surfaces in the usage environment, diffuses rapidly within the steel, segregates at lattice defects such as grain boundaries, and causes hydrogen embrittlement.[2] Therefore, understanding hydrogen diffusion behavior and the influence of alloying elements on it is extremely important in the material design of steels used in hydrogen environments.[33] However, experimentally investigating this requires considerable time. Therefore, we investigated the prediction of the effects of alloying elements on hydrogen diffusion using computational science.

Here, as a simplified system for austenitic steel used in hydrogen gas environments, we focused on predicting hydrogen diffusion in Ni-Mn alloys, which share the same fcc structure and for which experimental hydrogen diffusion data exist. For hydrogen diffusion in pure Ni, molecular dynamics calculations using an empirical interatomic potential, whose parameters were adjusted to be consistent with DFT, have been reported to quantitatively reproduce experimental hydrogen diffusion coefficient results.[34] However, constructing a high-precision empirical interatomic potential for the magnetic

Ni-Mn-H ternary system is difficult.[20] Furthermore, even in studies using MLIP, Ni-Mn alloys are typically assumed to be random alloys where Mn exists in a random arrangement within Ni,[9] and no examples existed of constructing a ternary MLIP capable of reproducing hydrogen diffusion behavior under the diverse atomic environments present in these alloys.

Therefore, we newly constructed an MLIP for the Ni-Mn-H ternary system. Using molecular dynamics calculations with this MLIP, we non-empirically predicted the hydrogen diffusion coefficient in the random alloy and verified its validity by comparing it with experimental results. For MLIP construction, we applied a novel active learning method[35] that incorporates a screening process based on atomic structural features, in addition to the active learning approach commonly used for MLIP construction based on the uncertainty of interatomic forces.[36] This method enabled efficient sampling of the diverse atomic environments that should be considered in analyzing hydrogen diffusion behavior in alloys, facilitating the construction of a highly accurate MLIP.

Details are omitted, but the obtained MLIP accurately reproduced DFT calculations concerning lattice constants of Ni-Mn alloys, hydrogen solid solution energy in Ni-Mn alloys, activation energy for diffusion, and other parameters essential for high-precision prediction of hydrogen diffusion coefficients. Using the obtained MLIP, an atomic structure model of a random alloy, as shown in **Fig. 5**, was constructed. Hydrogen atoms were placed in this model, and molecular dynamics calculations were performed to anneal the alloy isothermally in the range of 700–900 K. The mean squared displacement of hydrogen during annealing was calculated. The results were fitted using Einstein's equation to determine the hydrogen diffusion coefficient at each temperature. From the Arrhenius plots of the diffusion coefficients at each temperature, the prefactor and activation energy for hydrogen diffusion were calculated.

Figure 6 shows the relationship between the prefactor of the hydrogen diffusion coefficient and the activation energy as a function of Mn addition in Ni-Mn alloys, combining computational and experimental results. For pure Ni, experimental results reported by Omura et al.,[33] Katz et al.,[37] and Völkl et al.[38] are shown. Considering the scatter in the experimental data for pure Ni, the computational results reproduce the experimental results with extremely good accuracy. In particular, they well reproduce the nonlinear behavior of the activation energy and prefactor with increasing Mn content. Note that the calculated activation energies are systematically smaller than the experimental values; this is due to quantum effects not considered in the molecular dynamics calculations.[39]

Furthermore, a detailed analysis of Mn's effect based on the computational results revealed two opposing effects on hydrogen diffusion due to Mn addition: an increase in activation energy caused by direct interaction between Mn and hydrogen at the diffusion barrier position, and a decrease in activation energy due to lattice constant expansion. It became clear that the nonlinear behavior of the hydrogen diffusion coefficient arises because the dominant mechanism changes depending on the Mn addition amount.

As described above, the construction of a high-precision MLIP and molecular dynamics calculations using it enable the investigation of the influence of alloying elements on the hydrogen diffusion coefficient without conducting experiments.

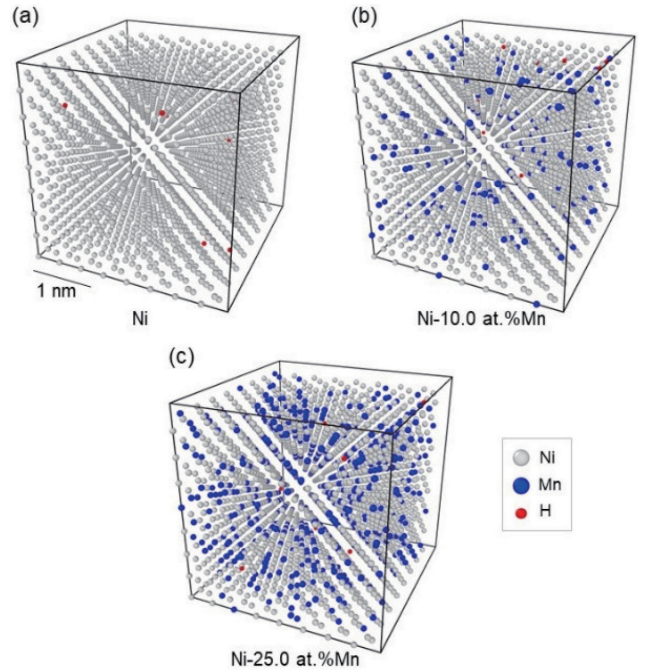

Fig. 5 Atomic structures used in molecular dynamics simulations for predicting hydrogen diffusion coefficients[27]
As examples, results for Ni, Ni–10.0 at.% Mn, and Ni–25.0 at.% Mn are shown. Gray, blue, and red spheres represent Ni, Mn, and H atoms, respectively.

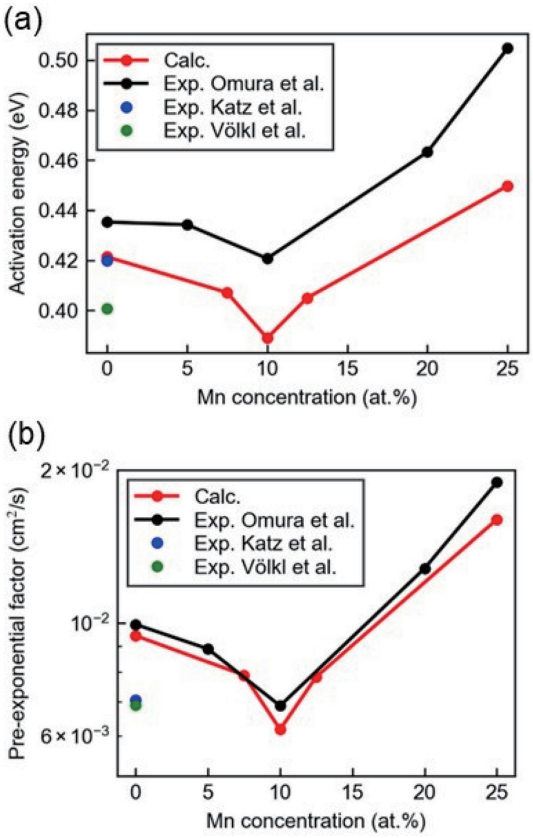

Fig. 6 Comparison of calculated hydrogen diffusion coefficients in Ni–Mn alloys with experimental values[27]
Effect of Mn addition on hydrogen diffusion in Ni: (a) activation energy and (b) pre-exponential factor. For comparison, experimental results reported by Omura et al.[33], Katz et al.[37], and Völkl et al.[38] are also shown.

4. Conclusion

The advent of MLIPs has enabled large-scale analysis with DFT-level accuracy. Recently, MLIPs have been constructed even for multinary systems like high-entropy alloys.[22] However, the accuracy for general grain boundaries containing complex atomic structures and their deformation behavior remains insufficiently guaranteed.[21]

Currently, within the Fugaku Industrial Project, we are working on constructing an MLIP for Fe multinary systems. Constructing an MLIP for Fe is more challenging than for other metals due to its magnetic properties. However, we have recently succeeded in constructing an MLIP for the Fe-H binary system that can handle deformation, fracture, and the influence of hydrogen at general grain boundaries with high precision.[40] Furthermore, by optimizing the MLIP framework and training conditions, we have successfully developed an Fe–H MLIP that achieves more than a tenfold increase in computational efficiency while maintaining the same level of accuracy.[41]

This technological field is advancing remarkably, and we believe high-precision analysis of multinary and large-scale systems will become possible in the near future. At that time, atomic-level computational methods will undoubtedly be indispensable for the development of steel materials.

Acknowledgments

Part of this research was conducted using computational resources provided by the supercomputer “Fugaku” (Project Numbers: hp230272, hp240280). Part of this research received support from the Research Organization for Information Science and Technology (RIST) through its accompanying utilization support program (Support IDs: 23Z-03, 23Z-05, 24H1-01; Support details: application porting, job submission, execution performance tuning, etc.).

References

1) Briant, C.L., Banerji, S.K.: Int. Mater. Rev. 23, 164–199 (1978)
2) Yu, H., Díaz, A., Lu, X., Sun, B., Ding, Y., Koyama, M., He, J., Zhou, X., Oudriss, A., Feaugas, X., Zhang, Z.: Chem. Rev. 124, 6271–6392 (2024)
3) Uenishi, A.: Nippon Seitetsu Giho. (412), 8–13 (2019)
4) Takayama, S., Ogura, T., Fu, S.-C., McMahon, C.J.: Metall. Trans. A. 11, 1513–1530 (1980)
5) Lejček, P., Šob, M., Paidar, V.: Prog. Mater. Sci. 87, 83–139 (2017)
6) Chen, Y.-S., Liu, P.-Y., Niu, R., Devaraj, A., Yen, H.-W., Marceau, R.K.W., Cairney, J.M.: Microsc. Microanal. 29, 1–15 (2023)
7) Dong, L., Wang, S., Wu, G., Gao, J., Zhou, X., Wu, H.-H., Mao, X.: Int. J. Hydrog. Energy. 47, 20288–20309 (2022)
8) Taniguchi, S., Kameya, M., Kobayashi, Y., Ito, K., Yamasaki, S.: ISIJ Int. 64, 1057–1066 (2024)
9) Ito, K., Yamamura, M., Omura, T., Yamabe, J., Matsunaga, H.: Int. J. Hydrog. Energy. 50, 148–164 (2024)
10) Ito, K., Omura, T., Udagawa, A., Takai, K.: Acta Mater. 304, 121807 (2026)
11) Ito, K., Sawada, H.: Comput. Mater. Sci. 210, 111050 (2022)
12) Ito, K.: Mater. Today Commun. 38, 107849 (2024)
13) Ito, K., Tanaka, Y., Tsutsui, K., Omura, T.: Comput. Mater. Sci. 218, 111951 (2023)
14) Ito, K., Tanaka, Y., Mitsunobu, T., Kohtake, T., Tsutsui, K., Sawada, H.: Phys. Rev. Mater. 6, 053604 (2022)
15) Ito, K., Mitsunobu, T., Ishiguro, Y., Kohigashi, Y., Tsutsui, K.: Phys. Rev. Mater. 6, 093603 (2022)
16) Ito, K., Tabata, S.-i.: Mater. Today Commun. 46, 112890 (2025)
17) Ito, K., Sawada, H., Ogata, S.: Mater. Trans. 62, 575–581 (2021)
18) Ito, K., Tanaka, Y., Sawada, H.: Mater. Trans. 63, 269-277 (2022)
19) Ito, K., Tanaka, Y., Tsutsui, K., Sawada, H.: Comput. Mater. Sci. 225, 112196 (2023)
20) Shiihara, Y., Kanazawa, R., Matsunaka, D., Lobzenko, I., Tsuru, T., Kohyama, M., Mori, H.: Scr. Mater. 207, 114268 (2022)
21) Mortazavi, B.: Adv. Energy Mater. 15, 2403876 (2025)
22) Wang, F., Wu, H.-H., Dong, L., Pan, G., Zhou, X., Wang, S., Guo, R., Wu, G., Gao, J., Dai, F.-Z., Mao, X.: J. Mater. Sci. Technol. 165, 49–65 (2023)
23) Szlachta, W.J., Bartók, A.P., Csányi, G.: Phys. Rev. B. 90, 104108 (2014)
24) Mortazavi, B., Zhuang, X., Rabczuk, T., Shapeev, A.V.: Mater. Horiz. 10, 1956–1968 (2023)
25) Ito, K., Yokoi, T., Hyodo, K., Mori, H.: Int. J. Mech. Sci. 291–292, 110132 (2025)
26) Ito, K., Yokoi, T., Hyodo, K., Mori, H.: Npj Comput. Mater. 10, 255 (2024)
27) Ito, K., Matsumura, N., Iwasaki, Y., Sakai, Y., Yamamura, M., Omura, T., Yamabe, J., Matsunaga, H.: Commun. Mater. 6, 195 (2025)
28) Meng, F.-S., Du, J.-P., Shinzato, S., Mori, H., Yu, P., Matsubara, K., Ishikawa, N., Ogata, S.: Phys. Rev. Mater. 5, 113606 (2021)
29) Poul, M., Huber, L., Bitzek, E., Neugebauer, J.: Phys. Rev. B. 107, 104103 (2023)
30) Shapeev, A.V.: Multiscale Modeling & Simulation. 14, 1153–1173 (2016)
31) Podryabinkin, E., Garifullin, K., Shapeev, A., Novikov, I.: J. Chem. Phys. 159, 084112 (2023)
32) Li, C., Lu, S., Divinski, S., Vitos, L.: Acta Mater. 255, 119074 (2023)
33) Omura, T., Yamamura, M., Ito, K., Yamabe, J., Matsunaga, H.: ISIJ Int. 65, 1402–1409 (2025)
34) Torres, E., Pencer, J., Radford, D.D.: Comput. Mater. Sci. 152, 374–380 (2018)
35) Matsumura, N., Yoshimoto, Y., Yamazaki, T., Amano, T., Noda, T., Ebata, N., Kasano, T., Sakai, Y.: J. Chem. Theory Comput. 21, 3832–3846 (2025)
36) Zhang, Y., Wang, H., Chen, W., Zeng, J., Zhang, L., Wang, H., Weinan, E.W.: Comput. Phys. Commun. 253, 107206 (2020)
37) Katz, L., Guinan, M., Borg, R.J.: Phys. Rev. B. 4, 330–341 (1971)
38) Völkl, J., Alefeld, G., in Hydrogen in Metals I: Basic Properties, eds. G. Alefeld and J. Völkl, Springer Berlin Heidelberg, Berlin, Heidelberg, 1978, pp. 321–348
39) Wimmer, E., Wolf, W., Sticht, J., Saxe, P., Geller, C.B., Najafabadi, R., Young, G.A.: Phys. Rev. B. 77, 134305 (2008)
40) Ito, K., Otaki, T., Hyodo, K., Yokoi, T., Mori, H.: Commun. Mater. 7, 30 (2026)
41) Ito, K.: Int. J. Hydrog. Energy. 242, 155600 (2026)

Kazuma ITO
Dr. Eng., Senior Researcher
Materials Characterization Research Lab.
Advanced Technology Research Laboratories
20-1 Shintomi, Futtsu City, Chiba Pref. 293-8511